The mass ratio and the orbital parameters of the sdOB binary AA Doradus

Slavek M. Rucinski⋆

Department of Astronomy, University of Toronto
50 St. George St., Toronto, Ontario, Canada M5S 3H4

ABSTRACT
The time sequence of 105 spectra covering one full orbital period of AA Dor has been analyzed. Direct determination of $V \sin i$ for the sdOB component from 97 spectra outside of the eclipse for the lines Mg II 4481 Å and Si IV 4089 Å clearly indicated a substantially smaller value than estimated before. Detailed modelling of line profile variations for 8 spectra during the eclipse for the Mg II 4481 Å line, combined with the out-of-eclipse fits, gave $V \sin i = 31.8 \pm 1.8$ km s^{-1}. The previous determinations of $V \sin i$, based on the He II 4686 Å line, appear to be invalid because of the large natural broadening of the line. With the assumption of the solid-body, synchronous rotation of the sdOB primary, the measured values of the semi-amplitude K_1 and $V \sin i$ lead to the mass ratio $q = 0.213 \pm 0.013$ which in turn gives K_2 and thus the masses and radii of both components. The sdOB component appears to be less massive than assumed before, $M_1 = 0.25 \pm 0.05 \, M_\odot$, but the secondary has its mass–radius parameters close to theoretically predicted for a brown dwarf, $M_2 = 0.054 \pm 0.010 \, M_\odot$ and $R_2 = 0.089 \pm 0.005 \, R_\odot$. Our results do not agree with the recent determination of Vǔcković et al. (2008) based on a K_2 estimate from line-profile asymmetries.

Key words: stars: binaries: close – binaries: eclipsing – stars: individual: AA Dor

1 INTRODUCTION

AA Doradus (LB 3459, HD 269696, $V \approx 11$) is a well known, close, short period (0.261 d), totally eclipsing binary consisting of a hot ($T_{eff} \approx 42,000 \, K$) sdOB, compact star and an invisible object. A recent review of Heber et al. (2008) gives a broad description of the sdB and sdO sub-dwarfs and of the intense research in this field.

The eclipses of the sdOB primary component of AA Dor are total and deep (≈ 0.35 mag). The illumination (reflection) effect from the invisible body is very strong and highly wavelength dependent: It is apparently mostly the heating effect as it is the strongest in IR and almost absent in UV; the secondary eclipses are entirely due to the eclipses of this additional, "reflected" light.

Previous investigations of AA Dor (Kilkenny et al. 1978, 1979; Hilditch et al. 1996, 2003; Rauch & Werner 2003) have resulted in an excellent and detailed description of its geometry in *relative* units: The relative radii ($r_1 = 0.1419$, $r_2 = 0.0764$) and the orbital inclination ($i = 89.2 \, \mathrm{deg}$) are known to a very high accuracy. However, the *absolute* parameters of AA Dor have not been known until the very recent paper of Vǔcković et al. (2008).

This is related to the single-lined (SB1) character of the spectrum which can provide only the semi-amplitude K_1 (Hilditch et al. 2003; Rauch & Werner 2003). Thus, the absolute sizes and masses could only be guessed using various reasonable assumptions on the mass of the visible star and/or the mass ratio. However, the sdOB component is not an average and typical star so such assumptions may be risky.

Vǔcković et al. (2008), through ingenious data processing of the same data as used in this paper, have been able to detect weak asymmetries in the hydrogen line wide wings. The asymmetric components were in emission and moved in anti-phase to the primary component motion permitting an estimate of K_2. In this paper we show that this determination does not agree with our entirely independent analysis based on the measured value of $V \sin i$ and the assumptions of the solid-body, synchronous rotation for the primary component.

2 OBSERVATIONAL DATA

The analysis presented here is based on the collection of 105 spectra obtained within the program of Rauch & Werner (2003) on January 8, 2001 using the 8m ESO telescope and
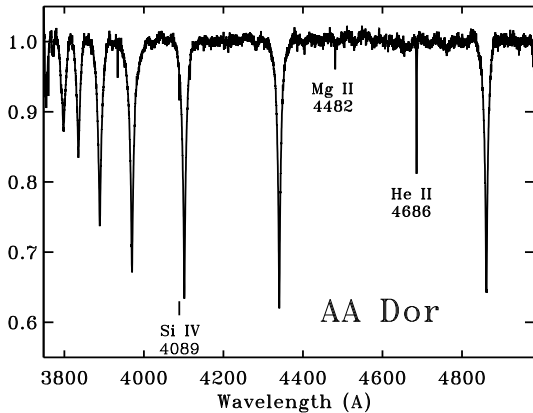
⋆ E-mail: rucinski@astro.utoronto.ca

Figure 1. The first of 105 spectra at the orbital phase 0.494, used in this analysis and taken here as an example. The three spectral lines used in this paper for $V \sin i$ determination are marked.

the UVES spectrograph. The observations became available to the author through the kindness of Dr. T. Rauch; they are accessible through the European Southern Observatory (ESO) archives.

The spectra were obtained in a somewhat cloudy weather (roughly 50% changes in the air transparency), over slightly more than one orbital cycle of the star, starting at orbital phases of the secondary eclipse (the hot star in front). The exposures were taken at equal intervals of 3.75 minutes. The nominal resolving power was $R \approx 48,000$, corresponding to 6.2 km s^{-1} (for a Gaussian profile, $\sigma_{instr} \approx 3.0$ km s^{-1}). The wavelength sampling of the spectra was 0.015 Å i.e. about 1 km s^{-1}. Although the AA Dor spectra have been fully reduced through the ESO pipeline and expressed in the heliocentric radial velocity system, no standard or calibration star spectra were provided. The remaining details are given in Rauch & Werner (2003).

Figure 1 shows the rectified spectrum AA Dor, the first of the 105 used; the average spectrum of AA Dor formed from the same observations is shown magnified in Figure 2 of Rauch & Werner (2003). The latter figure was used as a guidance during rectification of the spectra because the raw data showed relatively large, wave-like intensity variations of the order of 50% along the covered wavelength range.

Of note in Figure 1 are the very wide hydrogen lines extending in radial velocities over a few thousand km/s. The only obviously sharp and relatively deep (about 20 % depth) line is the He II 4686 Å line. This line was used by Rauch & Werner (2003) for a detailed modelling of the rotational broadening; however the intrinsic factors of the fine structure splitting and of a large thermal broadening (light atoms) gave only moderate quality results for the important quantity of the projected rotational velocity $V \sin i$. For that reason, we used much shallower but sharper lines of Mg II 4482 Å and Si IV 4089 Å in our determination of $V \sin i$ (Sections 4 − 6).

The extensive analysis of the ESO/UVES spectral series by Rauch & Werner (2003), while consistent with that of Hilditch et al. (2003), has not improved our knowledge of the system beyond providing the well defined value of $K_1 = 39.19 \pm 0.05$ km s^{-1} and a much less well defined $V_{rot} = 47 \pm 5$ km s^{-1} (note that the latter quantity has

the error one hundred times larger than the former). It is not clear if the latter value is the aspect-corrected one; Hilditch et al. (2003) used $V \sin i = 43 \pm 5$ km s^{-1}. Assuming a plausible range of the masses for the primary, $M_1 \approx 0.33 − 0.47 \, M_\odot$, and the value of K_1 as above, Hilditch et al. (2003) arrived at $M_2 \approx 0.064 − 0.082 \, M_\odot$ for the invisible object. While this was the best that could be derived, it definitely requires confirmation. We show in this paper that a targeted determination of $V \sin i$ may indicate a rather different set of absolute parameters of AA Dor.

Recently, after the analysis for this paper was concluded, a new determination of the rotational velocity of AA Dor appeared (Fleig et al. 2008). It is based on a detailed analysis of far ultraviolet spectra from the FUSE satellite. The new value is substantially smaller than used before, $V_{rot} = 35 \pm 5$ km s^{-1}, and better agrees with the results of this paper. However, our analysis uses a very different approach and results in a smaller uncertainty so it is useful as an entirely independent determination.

3   ROTATION VELOCITY OF THE PRIMARY COMPONENT AND THE PARAMETERS OF THE SYSTEM

The eclipsing binary system AA Dor has an excellent light-curve solution and the relative sizes of components are very well known (Hilditch et al. 2003). Yet, the physical scale of the system, which is needed for derivation of the masses requires not only the easily measurable semi-amplitude K_1 but also information on the motion of the secondary component. Although an estimate of K_2 has been recently found (Vǔcković et al. 2008), it may be biased as it was derived from tiny spectral-line asymmetries. Instead, we propose to utilize as the second quantity the value of the projected equatorial velocity of the primary star, $V \sin i$. One can then estimate the mass ratio of the system, $q = M_2/M_1$, and obtain a full description of the binary system in *physical units* by making the two assumptions about the primary component: (1) the solid-body rotation and (2) the perfect rotation–orbital motion synchronism. The ratio of the projected equatorial velocity to the observed orbital semi-amplitude,

$$V \sin i / K_1 = r_1(1 + 1/q) \qquad (1)$$

relates the relative size of the visible star (r_1) to the relative size of its orbit. This can be used to determine q and then $K_2 = K_1/q$.

While K_1 is relatively easy to find for AA Dor, $V \sin i$ has been poorly determined. We attempt to determine $V \sin i$ first by direct fits to the spectral line profiles (Section 4) and then by modelling of the line profile variations during eclipses of the primary (Section 5).

4   SPECTRAL LINE PROFILE ROTATIONAL FITS OUTSIDE OF ECLIPSES

There are very few sharp lines in the spectrum of AA Dor (the full spectrum of AA Dor is shown in Figure 2 of Rauch & Werner (2003)). The only visibly sharp and deep (20%) line is the He II 4686 Å line. The lines of Mg II 4481
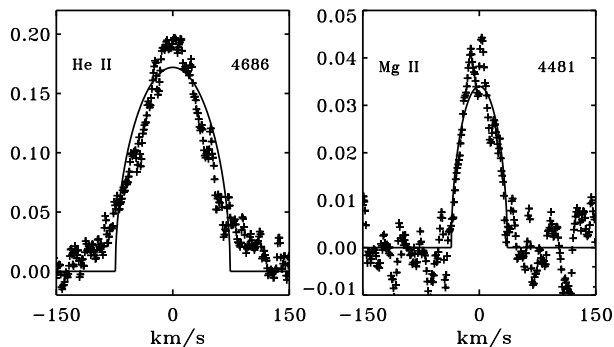
Figure 2. Two spectral lines of He II 4686 Å and Mg II 4481 Å, in the first spectrum of the series of 105 spectra, at the orbital phase 0.494 (the primary star in front). The rotational profile fits are for mean parameters established for all 97 out-of-eclipse spectra which were used for determinations of K_1 and $V \sin i$. The line profiles are shown inverted with the vertical scale representing the depth of the line relative the local continuum.

Å and Si IV 4089 Å have depths of about 4 – 5%. Other sharp lines are either interstellar or appear in the UV part of the spectrum where their groups would require detailed modelling of the mutual overlap and blending.

The He II 4686 Å line was modelled in detail by Rauch & Werner (2003) providing determinations of K_1 and of $V \sin i$. However, the line does not look rotationally broadened at all (Figure 2) so direct rotation profile fits are expected to give biased results. In spite of this, all 97 out-of-eclipse line profiles for this line were fitted by by the standard rotation profile (assuming the limb darkening of $u = 0.16$ which is appropriate for the high temperature of the star) to provide orbital velocities of the visible star and repeated determinations of $V \sin i$. The orbital solution for a circular orbit is: $K_1 = 39.41 \pm 0.13$ km s^{-1}, $T_0 = 2451917.15400 \pm 0.00016$. Because there were no standard star observations to relate to, the centre of mass velocity was determined but later adjusted to zero by the choice of the reference wavelength, $V_0 = 0 \pm 0.09$ km s^{-1}. The mean standard errors have been determined by the bootstrap sampling and are more realistic than ones given by the formal least-squares linear estimates. For the eclipse profile fits, we used a slightly different $T_0 = 2451917.15389 \pm 0.00019$ which is based on the weighted mean of the orbital solutions for the He II line and the Mg II line (see below). Relative to the values given by Rauch & Werner (2003), the adopted K_1 is slightly larger by 0.2 km s^{-1} but has a four times larger (and probably more realistic) error. The value of T_0 is shifted forward by 0.0012 d. The variable T_0 was included in the solution to account for an (unlikely) chance of spots or other asymmetries manifesting themselves only spectroscopically; obviously, an addition of one additional degree of freedom can only lower the quality of $V \sin i$ determination, but was done to stay conservative with the determination.

The value of the formally obtained rotation profile width of the He II line is $V \sin i = 74.9$ km s^{-1}. The error of the single determination is 1.5 km s^{-1} and error of the mean of 97 determinations is some ten times smaller; however, such an error of the mean estimate would not make allowance for the systematic departures of the fit and would reflect only the consistently same shape of the line profile at

all phases. Thus, we do not attach too much significance to the formal errors and note that the determination of $V \sin i$ is large; it obviously combines genuine rotation with other sources of broadening. The spectrograph resolution is characterized by $\sigma \approx 3$ km s^{-1} so that the dominant effect must come from the natural broadening of the He II line. The He ions are light so that for the temperature of the AA Dor primary, the Doppler thermal widths is expected to be relatively large, $\xi_0 \approx 16$ km s^{-1}. The line additionally shows multiple components of the fine structure splitting, as discussed in Rauch & Werner (2003), but even these two effects combined are not large enough. This indicates that the He II 4686 Å line, in spite of its sharp appearance – at least compared with the hydrogen lines – is not sharp enough for a $V \sin i$ determination.

The Mg II 4481 Å and Si IV 4089 Å lines are expected to be sharper than the helium line because their thermal Doppler broadening is $\xi_0 \approx 5.5 - 6$ km s^{-1}. When combined with the spectrograph resolution, we may expect their natural profile to have a width of $\approx 7 - 8$ km s^{-1}. The Mg II 4481 Å line is indeed much sharper than the He II line (Figure 2) and its broadening does appear to be dominated by rotation. Fits of the rotational profile to the line profiles outside of the eclipse gave $K_1 = 39.6 \pm 0.33$ km s^{-1} and $V \sin i = 36.1$ km s^{-1}; for the latter quantity the formal error of a single determination is 3.4 km s^{-1} and does not include any systematic deviations in the $V \sin i$ fits.

The third of the considered lines, Si IV 4089 Å, is located on the wide and curved wing of the H-δ line. The raw spectra had a sensitivity dip in this region by some 1/3 of the highest counts with an associated increase in the noise. The line is also slightly shallower than the Mg II 4481 Å line. For these reasons we would consider results for this line as less reliable than those for the Mg II 4481 Å line. Individual fits of the rotational profiles to all out-of-eclipse Si IV line profiles gave $V \sin i = 31.9$ km s^{-1}, with the formal error of a single determination of 2.4 km s^{-1}. The small value of $V \sin i$ may be partly due to the distortion of the baseline by the H-δ line wing, but indicates that this quantity cannot be large.

To summarize: The value of $V \sin i$ estimated from direct line-profile fits to the Mg II 4481 Å and Si IV 4089 Å lines is 36.1 and 31.9 km s^{-1}, respectively, with the latter determination much less reliable than the former. The fits for the He II 4686 Å line gave entirely unreliable results apparently due to strong natural broadening of the line. In the next sections, we will address the matter of separation of the natural broadening contribution from the $V \sin i$ estimates through utilization of the line-profile variations during eclipses.

5 PREDICTED SPECTRAL LINE-PROFILE VARIATIONS DURING ECLIPSES

For determination of $V \sin i$, one can utilize the spectral line profile variations as the secondary component of AA Dor scans the velocity field of the eclipsed sdOB component. Because the geometry of the binary is fully defined in the relative units of the mean separation, the line profile variations are relatively easy to predict for the case of the eclipsed body rotating as a solid-body, rotationally-synchronized star.
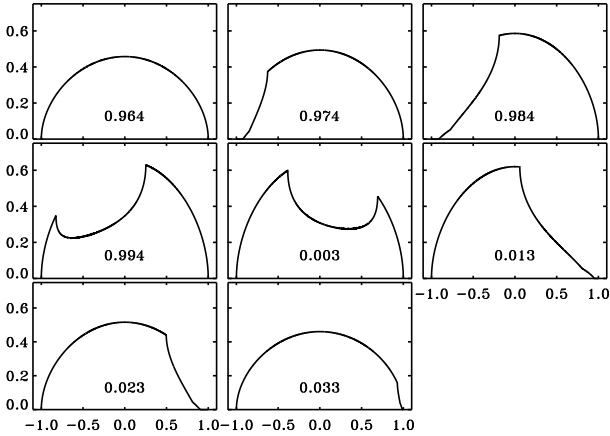
Figure 3. Predicted eclipse variations for an infinitely narrow spectral line in the spectrum of AA Dor during the primary eclipse. The X-axis is expressed in units of $V \sin i$ while the Y-axis is in arbitrary units but with the profiles normalized to give the same integral for all phases. The profiles have been calculated for eight observed phases as given by numbers in each panel.

The theoretical line profile variations during the eclipse (profiles called R below) calculated by direct integration over the uneclipsed portion of the primary star disk are shown for 8 eclipse phases of AA Dor in Figure 3. The X-axis in Figure 3 is in units of $V \sin i$ which is the free parameter of the problem. The profiles were computed for the limb darkening coefficient of $u = 0.16$ and then normalized to the total intensity of unity. This normalization is appropriate when the continuum for each phases is rectified and normalized to unity. The line profile variations are predicted to be enormous, a fact which may be used to determine the value of $V \sin i$. Such a determination would be independent of the out-of-eclipse line-shape fits which by necessity combine two similarly acting contributions of rotation and of natural line broadening.

The observed profile, $S(v)$, can be modelled by assuming that it is a convolution of the theoretical eclipse profile, $R(v - v_c; V \sin i)$ (such as in Figure 3), but shifted by the predicted orbital velocity of the primary mass centre v_c and stretched with the X-axis scale depending on $V \sin i$) with a natural-broadening profile, $N(v; p)$:

$$S(v) = \int R(v - v_c; V \sin i) \, N(v; p) \, dv \qquad (2)$$

The natural broadening is here meant to signify any contributions not related to rotation and thus not sensitive to eclipses, such as a combination of the Doppler thermal broadening with the spectrograph finite resolution. In the equation above, the integration variable is the radial velocity, v, while p is for any parameters used to describe the natural line broadening. The natural broadening can be assumed, for example, to be the velocity Doppler broadening $N \propto e^{-(v/\xi_0)^2}$, with the dispersion linked to the effective temperature T_{eff} and the atomic mass of the ion m through $\xi_0 = \sqrt{2 \mathcal{R} T_{eff}/m}$.

Fits of the $S(v)$ profiles to the observed ones must be done for all eclipse phases simultaneously, with (1) the same profile N (given explicitly or described by, say, a single parameter of the Doppler width), (2) a value of $V \sin i$

and (3) one scaling factor (when R is normalized to unit strength). With only three free parameters, the problem is a relatively simple one in terms of the parametric description, but somewhat complex for a solution because of the non-linear properties of the convolution operation. We describe below results of least-squares, non-linear fits for two spectral lines of He II 4686 Å and Mg II 4482 Å. Variations of the Si IV 4089 Å line were not modelled because of the curved baseline around this line caused by the Hδ wings and by the generally poorer definition of the spectrum in this region.

6   OBSERVED ECLIPSE VARIATIONS OF THE SPECTRAL LINE PROFILES

The He II 4686 Å line profile variations during the eclipse (Figure 4) are very unlike what is expected (Figure 3). This confirms that the natural broadening of this line totally dominates over the rotational broadening. The eclipse variations are almost invisible and the observed line – except for small centroid shifts and some changes in the overall width – looks practically the same at all eclipse phases. In a least-squares solution, the broadening profile had a tendency to evolve to a large value of $\xi_0 \approx 50$ km s^{-1}, with a very large uncertainty of ± 8 km s^{-1}. For such a choice, the best value of the rotational broadening is $V \sin i = 35$ km s^{-1}. The fits are reasonably good, but (1) because the eclipse effects are basically not present, the two broadenings simply combine (as they do outside of the eclipses); (2) the estimates of ξ_0 and $V \sin i$ are strongly anti-correlated with each determined to at best ± 8 km s^{-1}. We note that we have no explanation for the large width of the natural profile. This result casts a doubt on the previous determination of $V \sin i = 43 \pm 5$ km s^{-1} utilizing the He II 4686 Å line (Rauch & Werner 2003) and points at a need to use a narrower line. However, it agrees well with the recent determination of Fleig et al. (2008) of 35 ± 5 km s^{-1} from the FUSE data.

The Mg II 4481 Å line (Figure 5 gave the most reliable results. The linearized least-squares fits resulted in the Doppler width $\xi_0 = 13.8 \pm 0.4$ km s^{-1} and $V \sin i = 31.8 \pm 0.4$ km s^{-1}. The error estimates were obtained through bootstrap experiments over the whole ensemble of several thousand of data points; separate experiments utilizing re-sampling at the level of whole individual spectra suggest larger errors, ≈ 1.5 km s^{-1}. We note that the natural width is again substantially larger than expected.

The adopted $V \sin i$ for the visible star, determined as a weighted mean of our determinations, is $V \sin i = 31.8 \pm 1.8$ km s^{-1}. The estimate of the uncertainty takes into account the fact that the out-of-eclipse $V \sin i$ determinations in Section 4 are biased by the contribution of the instrumental as well as of the uncertain natural broadening; accordingly, they were given a low weight. We note that the values of ξ_0 that we were able to estimate from the line-profile eclipse variations turned larger than expected.

The value of $V \sin i$ is reduced by about one quarter relative to the previous determination of Rauch & Werner (2003) (43 km s^{-1}) and is even smaller than the more recent determination of Fleig et al. (2008) (35 km s^{-1}). This – together with the assumptions of the solid body, synchronous
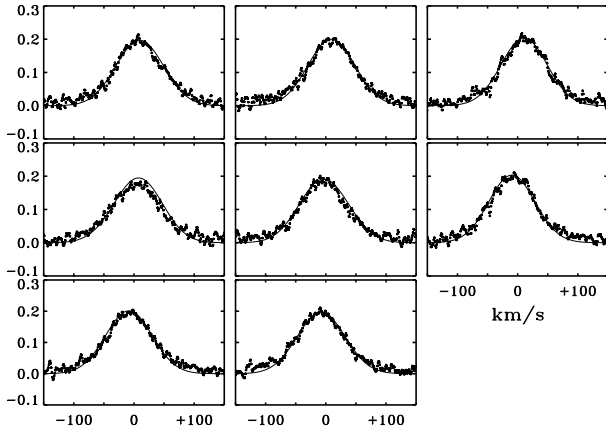
Figure 4. The line profile fits of the eclipse model to the He II 4686 Å line, for the same eight phases as in Figure 3. The global fit utilized only three free parameters (the best values in parentheses): (1) the natural, Gaussian broadening profile ($\xi_0 = 50$ km s^{-1}), (2) $V \sin i$ (35 km s^{-1}) and (3) a common scaling factor. The X-axis is in the observed radial velocities shifted to an arbitrary zero point while the Y-axis gives the inverted depth of the line.
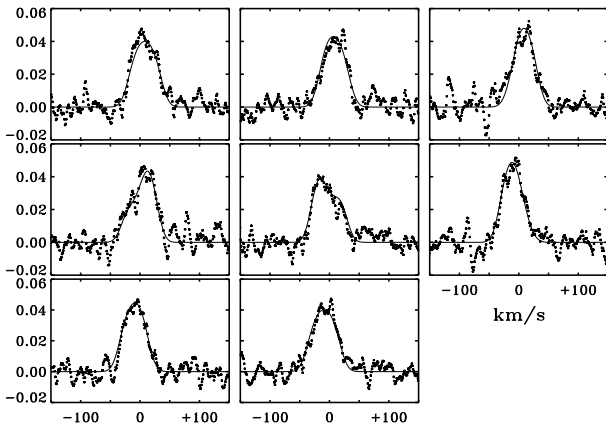

Figure 5. The line profile fits of our model to the Mg II 4481 Å line for the eight phases during the eclipse, the same as in Figures 3 and 4. The derived parameters are $V \sin i = 31.8$ km s^{-1} and the natural Gaussian broadening with $\xi_0 = 13.8$ km s^{-1}. Note that the vertical scale is much expanded relative to Figure 4 so that the noise is strongly visible, but that the horizontal scale is the same directly showing the lesser broadening of the Mg II 4481 Å line. Note also the detailed changes of this line, particularly for the central eclipse phases (panels 4 and 5).

rotation – leads to different orbital parameters of AA Dor than estimated before. This is discussed below.

7 PARAMETERS OF AA DOR

Having the value of $V \sin i$, we can determine the mass ratio q from Eq. 1 and then K_2. With the assumed inclination of the orbit from Hilditch et al. (2003), the resulting parameters of the binary system are as listed in Table 1. Note that in Table 1, we assumed a four times larger K_1 error than in the previous solutions, in accordance with the spread in

Table 1. Parameters of AA Dor

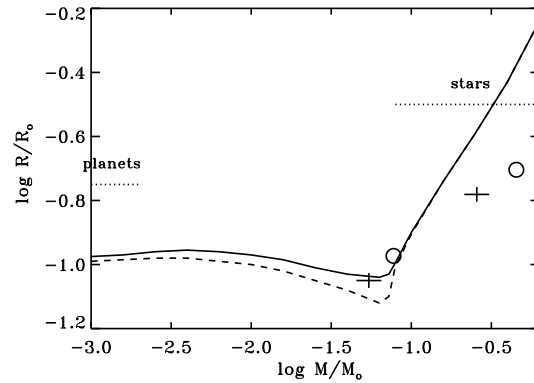| Parameter	Unit	Value	Std Error
P	day	0.261582	fixed
i	degree	89.2	fixed
$V \sin i$	km s^{-1}	31.8	1.8
K_1	km s^{-1}	39.4	0.2
K_2	km s^{-1}	184.7	12.3
$q = M_2/M_1$		0.213	0.013
$(M_1 + M_2) \sin^3 i$	$M_\odot$	0.305	0.055
M_1	$M_\odot$	0.251	0.046
M_2	$M_\odot$	0.054	0.010
$a \sin i$	$R_\odot$	1.158	0.070
R_1	$R_\odot$	0.165	0.009
R_2	$R_\odot$	0.089	0.005

Figure 6. The mass – radius relation for the solar composition (ages 1 Gyr and 10 Gyr) copied from Chabrier et al. (2008), with the two components of AA Dor marked by symbols. The crosses representing *formal* errors are for our determination while the circles are for the determination of Vučković et al. (2008). The dotted lines give the customary mass ranges for low-mass stars and massive planets. As expected, the sdOB primary is smaller than Main Sequence Stars, while the secondary appears to have parameters of an object at the border between brown dwarfs and low mass stars; the two solutions place it at both sides of the border.

the solutions based on the same data, as given in this paper and in Rauch & Werner (2003). This way, the disparity of errors of K_1 and $V \sin i$ appears to be more acceptable than in Rauch & Werner (2003) where they differed by a factor of one hundred times (0.05 and 5 km s^{-1}, respectively).

The solution as in Table 1 gives the mass of the primary sdOB component, $M_1 = 0.25 \pm 0.05\,M_\odot$, well outside the previously assumed and deemed plausible range of $0.33 - 0.47 M_\odot$ (Hilditch et al. 2003). This is not entirely surprising because the primary of AA Dor is thought to be a core of a much more massive star which underwent stripping in a common-envelope episode.

In contrast to the primary, the parameters of the secondary component are surprisingly "normal": With $M_2 = 0.054 \pm 0.010\,M_\odot$ and $R_2 = 0.089 \pm 0.005\,R_\odot$, this object appears to fully obey the mass – radius relation expected for brown dwarfs. In the recent discussion of the mass–radius relation by (Chabrier et al. 2008) only two objects with well determined parameters happen to be located in the domain

between the Main Sequence stars and Jupiter-like planets: Hat–P–2b and COROT–3b. The secondary of AA Dor appears at the very minimum of the radius in this relation, see Figure 6.

While we are satisfied by the results, there is a problem: They do not agree with the new determination of Vŭcković et al. (2008). Their direct estimate of $K_2 = 230$ km s^{-1} is substantially larger than our $K_2 = 185$ km s^{-1} so that both masses are larger than ours ($M_1 = 0.45\,M_\odot$ and $M_2 = 0.076\,M_\odot$). It is hard to imagine that the value derived by Vŭcković et al. (2008) is in some way biased by the illumination effect as then one would actually expect a *reduction* in K_2; however, the way how K_2 was estimated – through small line-profile asymmetries – does leave a wide margin of systematic uncertainty.

Our determination of the absolute parameters of AA Dor totally depends on the strong assumptions of the solid-body, synchronous rotation of the primary component. If any of these are not fulfilled, then our analysis is entirely invalid. The solid-body rotation assumption is – in principle – verifiable through analysis of the line-profile variations, but the current data are not accurate enough. We note that with the commonly agreed K_1 and with the new K_2 by Vŭcković et al. (2008), the expected $V\sin i = 38$ km s^{-1}, and this is entirely ruled out by our analysis. So, either our assumptions on the primary component rotation are invalid or the determination of Vŭcković et al. (2008) is biased. The case of AA Dor is still not closed.

REFERENCES

Chabrier, G., Baraffe, I., Leconte, J., Gallardo, J., Barman, T., 2008, arXiv: [astro-ph] 0810.5085

Fleig, J., Rauch, T., Werner, K., Kruk, J. W., 2008, A&A, 492, 565

Heber, U., 2008, in Hydrogen-Deficient Stars, ASP Conf, Vol.391; eds. K. Werner and T. Rauch; San Francisco: Astronomical Society of the Pacific, p.245

Hilditch, R. W., Kilkenny, D., Lynas-Gray, A. E., Hill, G., 2003, MNRAS, 344, 644

Hilditch, R. W., Harries, T. J., Hill, G., 1996, MNRAS, 279, 1380

Kilkenny, D., Hilditch, R. W., Penfold, J. E., 1978, MN-RAS, 183, 523

Kilkenny, D., Penfold, J. E., Hilditch, R. W., 1979, MN-RAS, 187, 1

Rauch, T., 2004, Rev. Mex. A. A., 20, 246

Rauch, T., Werner, K., 2003, A&A, 400, 271

Vŭcković, M., Østensen, R., Bloemen, S., Decoster, I., Aerts, C., 2008, in Hot Sudwarf Stars and Related Objects, ASP Conf, Vol.392; eds. U. heber, S. Jeffery, and R. Napiwotzki; San Francisco: Astronomical Society of the Pacific, p.199